Journal Pre-proof

Depletion of LAMP3 enhances PKA-mediated VASP phosphorylation to suppress invasion and metastasis in esophageal squamous cell carcinoma

Furong Huang, Gang Ma, Xuantong Zhou, Xiaolin Zhu, Xiao Yu, Fang Ding, Xiufeng Cao, Zhihua Liu

PII: S0304-3835(20)30133-6

DOI: https://doi.org/10.1016/j.canlet.2020.03.014

Reference: CAN 114738

To appear in: *Cancer Letters*

Received Date: 31 October 2019

Revised Date: 29 February 2020

Accepted Date: 15 March 2020

Please cite this article as: F. Huang, G. Ma, X. Zhou, X. Zhu, X. Yu, F. Ding, X. Cao, Z. Liu, Depletion of LAMP3 enhances PKA-mediated VASP phosphorylation to suppress invasion and metastasis in esophageal squamous cell carcinoma, *Cancer Letters*, https://doi.org/10.1016/j.canlet.2020.03.014.

Abstract

Metastasis is still a major cause of cancer-related mortality. Lysosome-associated membrane protein 3 (LAMP3) has been implicated in the invasiveness and metastasis of multiple cancer types; however, the underlying mechanisms are unclear. In this study, we found that *LAMP3* was overexpressed in esophageal squamous cell carcinoma (ESCC) tissues and that this increased expression positively correlated with lymph node metastasis. Depletion of LAMP3 dramatically suppressed the motility of ESCC cells *in vitro* and experimental pulmonary and lymph node metastasis *in vivo*. Importantly, knockdown of LAMP3 increased the level of phosphorylated VASP(Ser239), which attenuated the invasive and metastatic capability of ESCC cells. We identified that cAMP-dependent protein kinase A (PKA) was responsible for the phosphorylation of VASP at Ser239. Consistently, silencing of PKA regulatory subunits diminished Ser239 phosphorylation on VASP and restored the motility capacity of LAMP3-depleted ESCC cells. In conclusion, we uncovered a previously unknown role of LAMP3 in promoting cellular motility and metastasis in ESCC.

Keywords

LAMP3; VASP; PKA; Metastasis; Esophageal cancer

Abbreviations: LAMP3, lysosome-associated membrane protein 3; esophageal squamous cell carcinoma, ESCC; PKA, cAMP-dependent protein kinase A; LNM, lymph node metastasis.

Depletion of LAMP3 enhances PKA-mediated VASP phosphorylation to suppress invasion and metastasis in esophageal squamous cell carcinoma

Furong Huang[a, 1], Gang Ma[b, 1], Xuantong Zhou[a], Xiaolin Zhu[a], Xiao Yu[a], Fang Ding[a], Xiufeng Cao[c], Zhihua Liu[*a]

[a] State Key Laboratory of Molecular Oncology, National Cancer Center/National Clinical Research Center for Cancer/Cancer Hospital, Chinese Academy of Medical Sciences and Peking Union Medical College, Beijing 100021, PR China

[b] Department of Gastrointestinal Cancer Biology, Tianjin Medical University Cancer Institute and Hospital, National Clinical Research Center for Cancer, Key Laboratory of Cancer Prevention and Therapy, Tianjin 300060, PR China

[c] Department of Surgical Oncology, Nanjing First Hospital, Nanjing Medical University, Nanjing, Jiangsu 210029, PR China

[1] These authors contributed equally to this work.

* To whom correspondence should be addressed. Tel: +8610 87788490, Email: liuzh@cicams.ac.cn

Abstract

Metastasis is still a major cause of cancer-related mortality. Lysosome-associated membrane protein 3 (LAMP3) has been implicated in the invasiveness and metastasis of multiple cancer types; however, the underlying mechanisms are unclear. In this study, we found that *LAMP3* was overexpressed in esophageal squamous cell carcinoma (ESCC) tissues and that this increased expression positively correlated with lymph node metastasis. Depletion of LAMP3 dramatically suppressed the motility of ESCC cells *in vitro* and experimental pulmonary and lymph node metastasis *in vivo*. Importantly, knockdown of LAMP3 increased the level of phosphorylated VASP(Ser239), which attenuated the invasive and metastatic capability of ESCC cells. We identified that cAMP-dependent protein kinase A (PKA) was responsible for the phosphorylation of VASP at Ser239. Consistently, silencing of PKA regulatory subunits diminished Ser239 phosphorylation on VASP and restored the motility capacity of LAMP3-depleted ESCC cells. In conclusion, we uncovered a previously unknown role of LAMP3 in promoting cellular motility and metastasis in ESCC.

Keywords

LAMP3; VASP; PKA; Metastasis; Esophageal cancer

Abbreviations: LAMP3, lysosome-associated membrane protein 3; esophageal squamous cell carcinoma, ESCC; PKA, cAMP-dependent protein kinase A; LNM, lymph node metastasis.

1. Introduction

Metastasis is a leading cause of cancer-related death, as metastatic lesions are usually refractory to most treatment regimens and result in organ failures in the clinical setting. Although dozens of genes critical to cancer invasion and metastasis have been identified, the biological functions of these genes remain largely unexplored, which undoubtedly delays the development of novel anti-metastasis therapeutics in cancer. Therefore, further characterization of these metastasis-relevant genes would uncover potential targets to intervene in this lethal and complex process.

Lysosome-associated membrane proteins (LAMPs) are a family of membrane-bound glycosylated proteins in lysosomes. Five members (LAMP1, LAMP2, LAMP3/DC-LAMP, LAMP4, and LAMP5) have been identified, and all contain evolutionarily conserved LAMP domains [1]. Unlike ubiquitously expressed LAMP1 and LAMP2, *LAMP3* is expressed in specific cell types or in response to particular stimulations. Recently, several studies revealed that *LAMP3* overexpression positively correlates with poor prognosis in patients diagnosed with multiple cancer types [1]. The prometastatic function of LAMP3 was first uncovered in cervical cancer, which was supported by the observation that ectopic overexpression of *LAMP3* in the human cervical cancer cell line TCS enhanced cellular motility *in vitro* and metastasis *in vivo* [2]. When cervical cancer cells were under hypoxic conditions, the PERK/eIF2α/LAMP3 signaling axis was triggered in response to the activated unfolded protein response (UPR), and knockdown of LAMP3 inhibited hypoxia-

induced lymph node metastasis (LNM) [3]. Similar activity of LAMP3 was also observed in breast cancer, showing that hypoxia increased *LAMP3* expression via the PERK/ATF4 signaling pathway and further promoted migration in MDA-MB-231 cells [4]. Additionally, analysis of clinical samples from patients with breast cancer demonstrated that a high level of LAMP3 correlated with LNM [5]. Of note, it seems unlikely that the prometastatic function of LAMP3 is restricted to hypoxic stimulation. In head and neck squamous cell carcinoma (HNSCC), LAMP3 was found to be enriched in normoxic sections of tumors, and the increased protein level of LAMP3 was positively associated with LNM [6]. Thus, LAMP3 could enhance invasiveness and metastasis in multiple malignancies regardless of the normoxic or hypoxic state of tumor cells; however, the mechanisms of how LAMP3 regulates the motility of cancer cells are not clear.

A previous report documented that *LAMP3* expression increases in ESCC specimens compared with adjacent normal tissues, which indicates poor clinical outcomes in patients [7]. In this study, we found that depletion of LAMP3 markedly inhibited the motility and metastasis of two highly invasive ESCC cell sublines. Importantly, LAMP3 knockdown elicited increased levels of phosphorylated VASP at Ser239 specifically and suppressed cell motility *in vitro* and experimental metastasis *in vivo*. We identified that cAMP-dependent protein kinase A (PKA) facilitated VASP Ser239 phosphorylation in response to LAMP3 depletion. Altogether, we offer molecular insight into the promotility function of LAMP3 in ESCC cells.

2. Materials and methods

2.1. Cell culture

The human ESCC cell lines KYSE30 and KYSE450 were generously provided by Dr. Shimada Y. (Kyoto University, Kyoto, Japan) and maintained in RPMI 1640 medium supplemented with 10% fetal bovine serum (HyClone, South Logan, UT, USA). HEK293T cells were purchased from ATCC and cultured in DMEM supplemented with 10% fetal bovine serum. The ESCC sublines 30-D-4 and K450LM2 were generated from their corresponding parental cells in our laboratory as described previously [8]. All cells in this study were STR validated.

2.2. Antibodies and reagents

Commercially available antibodies in this study are as follows: anti-LAMP3 (ab153932 Abcam), anti-VASP (#3132 Cell Signaling Technology), anti-PRKAR1A (#3927 Cell Signaling Technology), anti-phospho-VASP (Ser157) (#3111 Cell Signaling Technology), anti-phospho-VASP (Ser239) (#3114 Cell Signaling Technology), anti-PRKAR2A (#10142-2-AP Proteintech), and anti-GAPDH (#2118 Cell Signaling Technology). cDNA clones were purchased from the following vendors: the LAMP3 ORF clone was from Origene (#SC115004, Rockville, MD, USA), and the VASP cDNA clone was from GeneCopoeia (EX-G0817-M98, Rockville, MD, USA). The inhibitors were purchased from Selleck Chemicals (Houston, TX, USA), including H 89 2HCl

(S1582), dorsomorphin (S7840), bithionol (S4552) and SQ22536 (S8283). G418 and puromycin were from Thermo Fisher Scientific (Waltham, MA, USA). D-Luciferin (#122799) was purchased from PerkinElmer (Waltham, MA, USA) and dissolved in DPBS (15 mg/mL).

2.3. Plasmid construction and lentivirus

LAMP3 and VASP cDNA were subcloned into the pLVX-IRES-neo vector. The VASP(S239A) mutant was generated with the primers listed in the Supplementary Table. Empty pLVX-IRES-neo was used as a negative control. Oligos targeting LAMP3, VASP, PRKAR1A or PRKAR2A were designed and constructed into pSIH-H1-puro (Supplemental Table). A nontargeting oligo was engineered into pSIH-H1-puro as a negative control.

For lentivirus production, the packaging plasmids and the indicated lenti-vectors were cotransfected into HEK293T cells. After transfection for 48 h, culture medium containing mature lentivirus particles was collected and stored in aliquots in a -80°C freezer. Cells were incubated with the indicated lentivirus and polybrene (1 μl/ml) for 24 h. G418 (400 μg/ml) or puromycin (2 μg/ml) was used to establish stable cell populations.

2.4. Clinical tissues and immunohistochemistry

The ESCC LNM tissue microarray was purchased from Outdo Biotech Company (#HEso-Squ127Lym-01, Shanghai, China). Esophageal cancerous and paired adjacent

normal tissues (N=26) were collected from the Department of Surgical Oncology in Nanjing First Hospital (Nanjing, China). The experimental procedures were approved by the ethical committee of the hospital, and informed consent was obtained from each enrolled patient.

The LNM tissue microarray was stained with anti-LAMP3 antibody (1:200) following the IHC procedure described previously [8]. IHC images were acquired and analyzed with an Aperio ImageScope system (Leica Biosystems, Buffalo Grove, IL, USA).

2.5. Cell viability assays

Cell proliferation was quantified by CCK-8 assays (#CK04, Dojindo Molecular Technologies, Japan). K450LM2 or 30-D-4 cells from the LAMP3 knockdown and control groups were seeded in 96-well plates (2×10^3 cells/well). CCK-8 was added to each well (10 μL/well) and incubated for 1 h. Absorbance at 450 nm was measured using a microplate reader (BioTek). The experiments were performed for three consecutive days.

2.6. Transwell assays

Either 30-D-4 cells (6×10^4 per insert) or K450LM2 cells (2×10^5 per insert) suspended in FBS-free RPMI 1640 medium were seeded into upper chambers with or without precoated Matrigel (BD, Franklin Lakes, NJ, USA). RPMI 1640 medium supplemented with 20% FBS in the bottom chambers acted as the chemotactic

agent. After a 24-h incubation, the migratory or invasive cells were fixed and stained with crystal violet. Cells in three randomly selected fields were photographed and counted.

2.7. RNA extraction and RT-qPCR

TRIzol (Thermo Fisher Scientific) was used to extract total RNA from the indicated cultured ESCC cells and the 26 pairs of ESCC/normal tissues according to the vendor's instructions. The cDNAs were obtained using a Quantscript RT kit (Tiangen, Beijing, China) following a previously described procedure [8]. The mRNA levels of *LAMP3* were detected using SYBR Premix Ex TaqTM II (TaKaRa, Japan) on a Step-one plus real-time PCR system (Applied Biosystems, Foster City, CA, USA). GAPDH was used for data normalization, and the $2^{-\Delta\Delta Ct}$ method was used to evaluate the relative abundance of LAMP3. Primers for LAMP3 and GAPDH are listed in the Supplementary Table.

2.8. Protein extraction and western blotting

Cellular total proteins were obtained under adherent or chemotactic conditions. In the case of chemotactic conditions, cells (5×10^5 cells per insert) were suspended in 1 ml of RPMI 1640 medium without FBS and seeded in the upper chambers (#3428, Corning). RPMI 1640 medium containing 20% FBS (2 ml per bottom chamber) was used as a chemotactic agent. Two hours after incubation at 37°C and 5% CO_2, the cells in the inserts were collected and lysed as was done for the

adherent cells. Cell lysis buffer (pH=7.4) consisted of 10 mM Tris-HCl, 150 mM NaCl, 5 mM EDTA, 1% Triton X-100, 0.25% sodium deoxycholate, and protease and phosphatase inhibitors (Roche). Western blotting assays were performed as described previously [8]. All immunoblot images were acquired by an ImageQuant LAS-4000 System (GE).

2.9. Animal experiments

In terms of the experimental lung metastasis model, 1 x 10^6 30-D-4 cells were injected into the tail veins of 6-week-old male SCID/Beige mice, which were provided by VitalRiver (Beijing, China). Mice were sacrificed 12 weeks after injection. For bioluminescence imaging, mice were anesthetized and injected with 10 μL/g D-luciferin in DPBS intraperitoneally. After 15 min, bioluminescence (BLI) was imaged via a Xenogen optical *in vivo* imaging system (IVIS; Xenogen). BLI was normalized to the background value, which was defined from luciferin-injected mice without tumor cells. To establish a murine LNM model, 5 x 10^5 30-D-4 cells were subcutaneously injected into the foot pads of 6-week-old male Balb/c nude mice. Mice were sacrificed approximately 10 weeks after injection. The harvested lungs or popliteal lymph nodes were paraffin-embedded and H&E stained to examine the metastatic lesions.

To test *in vivo* cellular growth, 1 x 10^6 shCtrl or shLAMP3 30-D-4 cells were subcutaneously injected into 6-week-old male Balb/c nude mice. The tumor sizes were measured every seven days. The tumor masses were harvested and weighed 35

days after the implantation. The volume of a tumor mass is calculated as (W^2 x L) / 2, where W is the width and L is the length. All animal studies were approved by the Institutional Animal Care and Use Committee of the Chinese Academy of Medical Sciences Cancer Hospital.

2.10. Statistical analysis

Data analysis was conducted using GraphPad Prism (Version 6). Each experiment, except the animal and IHC studies, was independently performed three times. The data are reported as the mean ± S.D. Statistical significance was calculated using two-sided Student's *t*-tests or the Wilcoxon matched-pairs signed rank test. ANOVA or the Friedman test was used for statistical analysis in multiple experimental groups. Statistical significance of positive LNM ratios in the indicated groups was determined by using the chi-square test. A P-value<0.05 was considered statistically significant.

3. Results

3.1. Increased LAMP3 expression in ESCC tissues positively correlates with invasiveness and metastasis

We first analyzed the mRNA level of *LAMP3* with two GEO datasets (GSE23400 and GSE20347), indicating that ESCC specimens displayed elevated levels of *LAMP3* mRNA compared with adjacent normal counterparts (Fig. 1A). We then examined a set of ESCC and paired adjacent normal tissues (N=26) to verify the *in silico* analysis results, confirming that *LAMP3* mRNA levels were upregulated in cancerous tissues

(Fig. 1A). As shown in Fig. 1B, *LAMP3* protein was mainly located in the cytoplasm and on the membrane of esophageal epithelial cells, and IHC scores of LAMP3 were markedly increased in ESCC tissues compared to those of paired normal specimens (N=77) (Fig. 1B and 1C). These results, which were consistent with previous findings, suggested that LAMP3 probably plays critical roles in ESCC progression [5, 6, and 7].

Since LAMP3 has been reported to promote invasiveness and metastasis in several solid tumors, a GEO dataset (GSE47404) relevant to LNM in patients with ESCC was used to examine whether LAMP3 functions in a similar way. We found that *LAMP3* mRNA was significantly increased in primary tumors from LNM-positive patients compared with LNM-negative patients (Fig. 1D). Additionally, LAMP3 was not or weakly stained in the negative lymph nodes (LNs), whereas metastatic ESCC cells in the positive LNs exhibited much stronger staining intensity (Fig. 1E). Accordingly, IHC scores of LAMP3 were strikingly higher in positive than in negative LNs (Fig. 1F). These results together indicate that *LAMP3* expression is aberrantly increased in ESCC cells and probably facilitates their invasion and metastasis.

3.2. LAMP3 promotes ESCC cell motility in vitro *without affecting cell viability*

We examined *LAMP3* expression in two pairs of ESCC cell lines in which highly invasive variants have been generated from parental cell lines in our laboratory: KYSE30, KYSE450 and their corresponding highly invasive sublines named after 30-D-4 and K450LM2 [8]. We found that *LAMP3* expression was markedly increased in both derivatives compared to their parental counterparts (Supplementary Fig. 1A and

1B). Given these results, we generated stable LAMP3-depleted 30-D-4 and K450LM2 cells using shRNA oligos targeting LAMP3 (shLAMP3#4/#6) or nontargeting shCtrl (Fig. 2A and 2B, Supplementary Fig. 1C and 1D). Meanwhile, KYSE30 and KYSE450 cells were infected with lentivirus to establish stable *LAMP3*-overexpressing (LAMP3) and control (pLVX) cell populations (Fig. 2C and 2D, Supplementary Fig. 1E and 1F).

By analyzing cell motility *in vitro*, we found that *LAMP3* knockdown dramatically suppressed the migration and invasion of 30-D-4 and K450LM2 cells. The number of penetrated cells decreased by at least 30% for shLAMP3#4/#6 30-D-4 cells and by more than 50% for shLAMP3#4/#6 K450LM2 cells compared to their counterparts in the shCtrl group (Fig. 2E and 2F). Wound healing assays further confirmed that LAMP3 deficiency reduced the number of 30-D-4 and K450LM2 cells that had migrated into the scratched wound after 36 h (Supplementary Fig. 1G and 1H). Conversely, *LAMP3* overexpression strongly enhanced the motility of KYSE30 and KYSE450 cells (Fig. 2G and 2H). Notably, LAMP3 depletion exhibited a modest effect on the viability of 30-D-4 or K450LM2 cells *in vitro,* as shown in CCK-8 assays (Supplementary Fig. 2A and 2B). We did not observe a significant difference in the growth of tumor masses arising from shLAMP3#4 or shCtrl 30-D-4 cells that were subcutaneously injected into male Balb/c nude mice (Supplementary Fig. 2C-E). Together, these data suggest that LAMP3 enhances ESCC cell migration and invasion *in vitro* without affecting cell viability.

3.3. LAMP3 promotes ESCC cell metastasis in vivo

Next, we investigated the roles of LAMP3 in ESCC metastasis *in vivo*. We injected luciferase-expressing shLAMP3#4/#6 and shCtrl 30-D-4 cells into the tail veins of male SCID/Beige mice (N=6 in each group). Pulmonary metastases were detected after 85 days, showing markedly decreased bioluminescence in the shLAMP3#4/#6 group compared to that in the shCtrl group (Fig. 3A). Overt metastatic nodes in the harvested lungs were also counted, and the average number of metastases dropped from approximately 140 in the shCtrl group to approximately 50 in the shLAMP3#4/#6 group (Supplementary Fig. 3A and 3B). Pathohistologic examination of these lungs demonstrated that the sizes of metastases arising from shLAMP3#4/#6 30-D-4 cells significantly diminished compared with the control counterparts (Fig. 3B). In addition, we subcutaneously inoculated shCtrl and shLAMP3#4/#6 30-D-4 cells into the foot pads of male Balb/c nude mice (N=8 in each group) (Fig. 3C). Popliteal LNs were collected and weighed. We found that popliteal LNs from the shCtrl group were larger and heavier than those from the shLAMP3#4/#6 group (Fig. 3D). Importantly, the ratios of positive popliteal LNMs were also significantly reduced from 100% (8/8) in the shCtrl group to 37.5% (3/8) in the shLAMP3#4 group and 50% (4/8) in the shLAMP3#6 group (Fig. 3E and 3F). Altogether, these results evidently show that depletion of LAMP3 impairs the metastatic capability of ESCC cells in both proximal popliteal lymph nodes and distal pulmonary tissues.

3.4. Depletion of LAMP3 elicits phosphorylation of its downstream effector VASP at Ser239

Protein phosphorylation changes are largely implicated in the cell signaling network, regulating normal physiological functions and pathologic conditions, notably cancers [9, 10]. The phosphorylation states of key proteins controlling the cell migration and invasion cascade were detected to explore the molecular mechanisms underlying LAMP3-mediated ESCC metastasis. We did not observe that depletion of LAMP3 significantly altered the levels of phosphorylated VASP at specific residues when 30-D-4 and K450LM2 cells were constantly adherent in the culture dishes (Supplementary Fig. 4A and 4B). However, LAMP3 knockdown markedly increased the phosphorylation of Ser239 on VASP in 30-D-4 cells that were under chemotaxis conditions (Fig. 4A). The level of phosphorylated VASP at Ser157 was measured as well, yet no change was found between shLAMP3#4/#6 and shCtrl 30-D-4 cells (Fig. 4A). Similar results were also detected in LAMP3-depleted K450LM2 cells compared with shCtrl counterparts (Fig. 4A). Otherwise, phosphorylation of Ser239 on VASP was attenuated by *LAMP3* overexpression in KYSE30 and KYSE450 cells (Fig. 4B).

It has been appreciated that diverse VASP functions are tightly governed by phosphorylation at distinct amino acid residues, among which Ser239 phosphorylation primes this protein for perturbing cell motility [11]. The aforementioned results thereby indicate that VASP is probably implicated in cell motility mediated by LAMP3 in ESCC cells. *VASP* expression was reduced via shRNAs (shVASP) in 30-D-4 or K450LM2 cells, and the migration and invasion capabilities *in vitro* were analyzed. When VASP was depleted, 30-D-4 cells manifested enhanced

motility, as demonstrated by the number of penetrated shVASP cells doubling relative to shCtrl cells (Fig. 4C and 4D). Likewise, the membrane-penetrated K450LM2 cells increased by approximately 25% as a result of VASP knockdown (Fig. 4E and 4F). To verify whether VASP acted downstream of LAMP3, we reduced *VASP* expression in shLAMP3 30-D-4 cells and then evaluated the migration and invasion in cells from the shCtrl, shLAMP3, and shLAMP3/shVASP groups (Fig. 4G). As shown in Fig. 4H, the motility capability of 30-D-4 cells was dramatically attenuated upon LAMP3 knockdown, whereas it was restored to a large extent when VASP was further depleted. Moreover, we also generated dual knockdown of LAMP3/VASP in K450LM2 cells and found that additional depletion of VASP completely rescued the motility ability of K450LM2 cells compared with knockdown of LAMP3 alone (Fig. 4I and 4J).

3.5. Phosphorylation of Ser239 on VASP is indispensable for inhibiting ESCC cell motility and metastasis

As we found that the level of phosphorylated VASP(Ser239) increased due to LAMP3 knockdown, lentivirus overexpressing wild-type VASP(WT), its point mutant VASP(S239A) and control lentivirus (pLVX) were generated to examine whether Ser239 is a critical residue involved in suppressing ESCC cell invasion and metastasis. Under chemotaxis conditions, shLAMP3 30-D-4 cells infected with VASP(WT) manifested markedly elevated phosphorylated VASP(Ser239), while the phosphorylation level of VASP at Ser239 in shLAMP3/VASP(S239A) cells was reverted to a comparable levels as that in shLAMP3/pLVX cells (Fig. 5A). We did not observe

that the migration and invasion ability decreased in shLAMP3/VASP(WT) 30-D-4 cells compared with shLAMP3/pLVX cells; however, the number of penetrated cells significantly increased when VASP(S239A) was forcedly expressed in shLAMP3 cells (Fig. 5B). The results acquired from K450LM2 cells highly resembled those in 30-D-4 cells (Fig. 5C and 5D). Together, these results indicate that mutation of Ser239 on VASP could strikingly reverse the motility inhibition exerted by LAMP3 knockdown in ESCC cells, and endogenous VASP is probably sufficient in this process.

We then determined whether Ser239 is also essential in LNM of ESCC cells. As shown in Fig. 5E, the sizes and weights of the popliteal LNs from the shLAMP3/pLVX and shLAMP3/VASP(WT) groups dramatically decreased compared with their counterparts from the shCtrl/pLVX group. Additionally, the popliteal LNs in the shLAMP3/VASP(S239A) group were significantly larger and heavier than those in the shLAMP3/pLVX and shLAMP3/VASP(WT) groups; however, no significant difference was identified between the LNs from the shCtrl/pLVX and shLAMP3/VASP(S239A) groups (Fig. 5E). H&E staining showed more metastatic lesions in the shCtrl/pLVX and shLAMP3/VASP(S239A) groups than in the shLAMP3/pLVX or shLAMP3/VASP(WT) groups (Fig. 5F). Importantly, the ratios of positive popliteal LNMs were significantly reduced from 100% (6/6) in the shCtrl group to 50% (3/6) in the shLAMP3/pLVX group and 33.3% (2/6) in the shLAMP3/VASP(WT) group, while the positive LNM ratio returned to 100% (6/6) in the shLAMP3/VASP(S239A) group, further demonstrating that VASP(S239A) enhances the ability of ESCC cells to give rise to overt metastases in LNs (Fig. 5G). All the data presented in Fig. 4 and Fig. 5 suggest

that VASP is a direct downstream effector of LAMP3, as Ser239 phosphorylation increases in response to depletion of LAMP3.

3.6. cAMP-dependent protein kinase A (PKA) phosphorylates Ser239 on VASP in ESCC cells

Previous studies showed that PKA and AMP-activated protein kinase (AMPK) are two major kinases that phosphorylate VASP at Ser239 [11]. To identify which kinase is responsible for phosphorylating VASP at Ser239, we treated ESCC cells with specific inhibitors targeting AMPK (dorsomorphin) or PKA (H 89 2HCL) to assess the VASP phosphorylation state under chemotaxis conditions. We found that the motility of dorsomorphin-treated shCtrl 30-D-4 cells was markedly attenuated compared with DMSO-treated counterparts, whereas H 89 2HCL markedly increased the number of penetrated shCtrl cells relative to their counterparts in the DMSO group (Fig. 6A). Intracellular PKA is activated by the local cAMP level, whose generation is catalyzed by adenylyl cyclases (ACs). SQ22536, which specifically inhibits the activity of ACs, enhanced the motile ability of shCtrl 30-D-4 cells (Fig. 6A). In contrast, we observed that bithionol, which deactivates only one soluble form of AC in mammals, decreased the number of penetrated shCtrl cells, suggesting that other membrane-bound ACs are probably instrumental in the inhibitory functions of PKA in ESCC metastasis (Fig. 6A). Notably, shLAMP3#4/#6 cells treated with H 89 2HCL or SQ22536 manifested relatively similar invasive ability compared to shCtrl cells exposed to the same inhibitors, indicating that these two inhibitors could antagonize the inhibitory effect

induced by LAMP3 depletion (Fig. 6A). Additionally, LAMP3 depletion failed to increase the level of phosphorylated VASP (Ser239) in H 89 2HCL- and SQ22536-treated cells (Fig. 6B).

The association between regulatory (R) subunits and A-kinase-anchoring proteins (AKAPs) direct the PKA-AKAP complex to distinct subcellular localizations [12]. Thus, diverse functions of PKA are spatially controlled. As AKAPs that are implicated in motility vary in different cell types [13, 14], we simultaneously reduced the expression of *PRKAR1A* encoding RIα and *PRKAR2A* producing RIIα in shLAMP3 30-D-4 and K450LM2 cells. Consistently, dual knockdown of PRKAR1A/2A decreased the level of phosphorylated VASP(Ser239), which to some extent restored the motile capability of shLAMP3 30-D-4 cells (Fig. 6C and 6D). The same results were also observed in LAMP3-depleted K450LM2 cells, showing that dual knockdown of these two R subunits dramatically restored the migration and invasion capacity of shLAMP3 K450LM2 cells compared to that of shCtrl counterparts (Fig. 6E and 6F). Together, these data demonstrate that local PKA phosphorylates VASP at Ser239 to negatively regulate the motility of ESCC cells under chemotaxis.

4. Discussion

It is beginning to be appreciated that metastasis is a systematic and highly dynamic process in which cancer cells are motivated to exploit almost all cellular

machinery [15]. Lysosomes contain plenty of hydrolytic enzymes, which are responsible for degrading proteins, lipids, and saccharides. Beyond acting as recycling centers of macromolecules, lysosomes also play critical roles in diverse malignant progressions, including invasion and metastasis [16]. Previous investigations have focused on lysosome-derived cathepsins and heparanase, which degrade the extracellular matrix, remodel the cellular membrane, and facilitate local invasion and distal metastasis accordingly [17, 18]. LAMP3 is a heavily glycosylated membrane protein in lysosomes and was recently uncovered to promote invasion and metastasis. Mechanistically, most studies have focused on the upstream regulation of *LAMP3* expression. Recently, an epigenetic mechanism regulating LAMP3 expression in ESCC revealed that the lncRNA HAGLR sponged miR-143-5p to inhibit its role in repressing LAMP3 expression [19]. Nevertheless, the underlying mechanisms of the involvement of LAMP3 in metastasis remain poorly understood. In this study, we found that knockdown of LAMP3 suppresses ESCC cell invasion and metastasis by enhancing the phosphorylation of VASP at Ser239 (Fig. 2-3, Fig. 4A-B). Mutated VASP(S239A) confers stronger motility capacity to ESCC cells (Fig. 5). We further identified that PKA is primarily responsible for phosphorylating VASP at Ser239, and inhibition of PKA activity enhances ESCC motility *in vitro* (Fig. 6). Collectively, LAMP3 promotes invasion and metastasis of ESCC cells by attenuating PKA-mediated phosphorylation of Ser239 on VASP.

VASP is one of the three members of the mammalian Ena/VASP protein family. In motile cells, VASP promotes assembly and elongation of F-actin stress fibers; thus, it

is usually enriched in focal adhesions and filopodia at the leading edge [11]. The subcellular localization and functions of VASP are controlled by phosphorylation at distinct residues, among which phosphorylated Ser157 guides VASP to reside in the leading edge and phosphorylation of Ser239 impairs F-actin bundling and filopodia formation [20]. We observed that VASP phosphorylation at Ser239 is dramatically increased due to LAMP3 depletion, whereas the level of phosphorylated VASP Ser157 remains comparable between shCtrl and shLAMP3 cells, suggesting that LAMP3 deficiency prevents actin filament formation without affecting the localization of VASP in ESCC cells (Fig. 4A-B). The inhibitory effect of phosphorylated VASP at Ser239 on the invasion and metastasis of ESCC cells was further verified (Fig. 5), which is concordant with previous findings and confirms that VASP is a downstream effector of LAMP3 [21, 22, 23]. Notably, the LAMP3-VASP axis could only be detectable when ESCC cells were under chemotaxis conditions, strongly suggesting that motile cells under chemotaxis conditions harbor molecular properties distinct from those of adherent cells.

LAMP3 does not possess kinase activity, thereby prompting us to identify potential kinases to phosphorylate Ser239 on VASP. PKA and AMPK have been described previously to add a phosphate group to Ser239 [11]. We found that PKA, not AMPK, is essential for phosphorylating VASP at Ser239 under chemotaxis (Fig. 6). Inactive PKA is a heterotetramer consisting of two catalytic (C) subunits and a dimer of regulatory (R) subunits. Activation of this kinase is triggered by cAMP binding to R subunits, and functional C subunits are released from the tetramer accordingly [24].

Four regulatory isoforms of PKA (RIα, RIβ, RIIα, and RIIβ) have been identified to provide docking sites for diverse AKAPs, which further bring PKA, substrates and phosphatases in close proximity, thus regulating the PKA signaling axis spatially and temporally to confer specificity and versatility to this pathway [12]. As expected, knockdown of *PRKAR1A* and *PRKAR2A* encoding RIα and RIIα, respectively, rescued the migration and invasion of ESCC cells in the shLAMP3 group (Fig. 6C-F).

One plausible association between LAMP3 and the PKA signaling pathway is that LAMP3 depletion may disturb the lysosomal degradation of key components in the PKA signaling axis. A previous report found that one LAMP2 isoform, LAMP-2A, recognizes amino acid sequences within specific proteins to deliver them into lysosomes [25]. Therefore, an intriguing assumption arises that LAMP3 is capable of binding to specific motifs on candidate proteins and transporting them into lysosomes. Interestingly, we found that LAMP3 depletion increased the protein level of *WAVE-1* in 30-D-4 and K450LM2 cells, which is an important AKAP to regulate the reorganization of the cytoskeleton and cellular motility (data not shown). Moreover, a co-IP assay showed that LAMP3 could physically bind WAVE-1 (data not shown). These preliminary results imply that LAMP3 probably recognizes and delivers some specific proteins into lysosomes for degradation. The investigations are in progress to test this hypothesis.

In conclusion, our findings reveal that the lysosome-associated protein LAMP3 plays essential roles in ESCC metastasis. LAMP3 deficiency inhibits ESCC metastasis by activating PKA-mediated VASP phosphorylation at Ser239 (Figure 7). As lysosomes

are involved in the degradation and recycling of proteins, systemic characterization of potential targets of LAMP3 is required to deepen the insight into its roles in metastasis.

Conflicts of interest

No potential conflicts of interest were disclosed.

Acknowledgments

This work was supported by National Key R&D Program of China (2016YFC1302100), and the CAMS Innovation Fund for Medical Sciences (2016-I2M-1-001, 2019-I2M-1-003).

References

[1] F. Alessandrini, L. Pezze, Y. Ciribilli, LAMPs: Shedding light on cancer biology, Seminars in oncology, 44 (2017) 239-253.

[2] H. Kanao, T. Enomoto, T. Kimura, M. Fujita, R. Nakashima, Y. Ueda, Y. Ueno, T. Miyatake, T. Yoshizaki, G.S. Buzard, A. Tanigami, K. Yoshino, Y. Murata, Overexpression of LAMP3/TSC403/DC-LAMP promotes metastasis in uterine cervical cancer, Cancer research, 65 (2005) 8640-8645.

[3] H. Mujcic, A. Nagelkerke, K.M. Rouschop, S. Chung, N. Chaudary, P.N. Span, B. Clarke, M. Milosevic, J. Sykes, R.P. Hill, M. Koritzinsky, B.G. Wouters, Hypoxic

activation of the PERK/eIF2alpha arm of the unfolded protein response promotes metastasis through induction of LAMP3, Clinical cancer research : an official journal of the American Association for Cancer Research, 19 (2013) 6126-6137.

[4] A. Nagelkerke, J. Bussink, H. Mujcic, B.G. Wouters, S. Lehmann, F.C. Sweep, P.N. Span, Hypoxia stimulates migration of breast cancer cells via the PERK/ATF4/LAMP3-arm of the unfolded protein response, Breast cancer research : BCR, 15 (2013) R2.

[5] A. Nagelkerke, H. Mujcic, J. Bussink, B.G. Wouters, H.W. van Laarhoven, F.C. Sweep, P.N. Span, Hypoxic regulation and prognostic value of LAMP3 expression in breast cancer, Cancer, 117 (2011) 3670-3681.

[6] A. Nagelkerke, F.C. Sweep, H. Stegeman, R. Grenman, J.H. Kaanders, J. Bussink, P.N. Span, Hypoxic regulation of the PERK/ATF4/LAMP3-arm of the unfolded protein response in head and neck squamous cell carcinoma, Head & neck, 37 (2015) 896-905.

[7] X. Liao, Y. Chen, D. Liu, F. Li, X. Li, W. Jia, High Expression of LAMP3 Is a Novel Biomarker of Poor Prognosis in Patients with Esophageal Squamous Cell Carcinoma, International journal of molecular sciences, 16 (2015) 17655-17667.

[8] G. Ma, C. Jing, L. Li, F. Huang, F. Ding, B. Wang, D. Lin, A. Luo, Z. Liu, MicroRNA-92b represses invasion-metastasis cascade of esophageal squamous cell carcinoma, Oncotarget, 7 (2016) 20209-20222.

[9] M. Grimes, B. Hall, L. Foltz, T. Levy, K. Rikova, J. Gaiser, W. Cook, E. Smirnova, T. Wheeler, N.R. Clark, A. Lachmann, B. Zhang, P. Hornbeck, A. Ma'ayan, M. Comb, Integration of protein phosphorylation, acetylation, and methylation data sets to

outline lung cancer signaling networks, Science signaling, 11 (2018).

[10] G. Xue, D.F. Restuccia, Q. Lan, D. Hynx, S. Dirnhofer, D. Hess, C. Ruegg, B.A. Hemmings, Akt/PKB-mediated phosphorylation of Twist1 promotes tumor metastasis via mediating cross-talk between PI3K/Akt and TGF-beta signaling axes, Cancer discovery, 2 (2012) 248-259.

[11] H. Doppler, P. Storz, Regulation of VASP by phosphorylation: consequences for cell migration, Cell adhesion & migration, 7 (2013) 482-486.

[12] K. Tasken, E.M. Aandahl, Localized effects of cAMP mediated by distinct routes of protein kinase A, Physiological reviews, 84 (2004) 137-167.

[13] A. A. Paulucci-Holthauzen, L. A. Vergara, L. J. Bellot, D. Canton, J. D. Scott, K. L. O'Connor, Spatial distribution of protein kinase A activity during cell migration is mediated by A-kinase anchoring protein AKAP Lbc, The Journal of biological chemistry, 9 (2009): 5956-5967.

[14] F. M. Tonucci, E. Almada, C. Borini-Etichetti, A. Pariani, F. Hidalgo, M. J. Rico, J. Girardini, C. Favre, J. R. Goldenring, M. Menacho-Marquez, M. C. Larocca, Identification of a CIP4 PKA phosphorylation site involved in the regulation of cancer cell invasiveness and metastasis, Cancer letters, 461 (2019): 65–77.

[15] Y. Suhail, M.P. Cain, K. Vanaja, P.A. Kurywchak, A. Levchenko, R. Kalluri, Kshitiz, Systems Biology of Cancer Metastasis, Cell systems, 9 (2019) 109-127.

[16] S.M. Davidson, M.G. Vander Heiden, Critical Functions of the Lysosome in Cancer Biology, Annual review of pharmacology and toxicology, 57 (2017) 481-507.

[17] M.M. Mohamed, B.F. Sloane, Cysteine cathepsins: multifunctional enzymes in

cancer, Nature reviews Cancer, 6 (2006) 764-775.

[18] G. Arvatz, I. Shafat, F. Levy-Adam, N. Ilan, I. Vlodavsky, The heparanase system and tumor metastasis: is heparanase the seed and soil?, Cancer metastasis reviews, 30 (2011) 253-268.

[19] C. Yang, S. Shen, X. Zheng, K. Ye, Y. Sun, Y. Lu, H. Ge, Long noncoding RNA HAGLR acts as a microRNA-143-5p sponge to regulate epithelial-mesenchymal transition and metastatic potential in esophageal cancer by regulating LAMP3, FASEB journal : official publication of the Federation of American Societies for Experimental Biology, 33 (2019) 10490-10504.

[20] P.M. Benz, C. Blume, S. Seifert, S. Wilhelm, J. Waschke, K. Schuh, F. Gertler, T. Munzel, T. Renne, Differential VASP phosphorylation controls remodeling of the actin cytoskeleton, Journal of cell science, 122 (2009) 3954-3965.

[21] D.S. Zuzga, J. Pelta-Heller, P. Li, A. Bombonati, S.A. Waldman, G.M. Pitari, Phosphorylation of vasodilator-stimulated phosphoprotein Ser239 suppresses filopodia and invadopodia in colon cancer, International journal of cancer, 130 (2012) 2539-2548.

[22] V. Gkretsi, D.P. Bogdanos, Experimental evidence of Migfilin as a new therapeutic target of hepatocellular carcinoma metastasis, Experimental cell research, 334 (2015) 219-227.

[23] N. Lund, D. Henrion, P. Tiede, M. Ziche, H. Schunkert, W.D. Ito, Vimentin expression influences flow dependent VASP phosphorylation and regulates cell migration and proliferation, Biochemical and biophysical research communications,

395 (2010) 401-406.

[24] C. Kim, D. Vigil, G. Anand, S.S. Taylor, Structure and dynamics of PKA signaling proteins, European journal of cell biology, 85 (2006) 651-654.

[25] K.E. Murphy, A.M. Gysbers, S.K. Abbott, A.S. Spiro, A. Furuta, A. Cooper, B. Garner, T. Kabuta, G.M. Halliday, Lysosomal-associated membrane protein 2 isoforms are differentially affected in early Parkinson's disease, Movement disorders : official journal of the Movement Disorder Society, 30 (2015) 1639-1647.

Figure Legends

Fig. 1 Overexpression of *LAMP3* in ESCC tissue positively correlates with LNM. **(A)** The mRNA level of *LAMP3* was analyzed in two independent ESCC patient cohorts, GSE23400 (left panel) and GSE20347 (middle panel), and 26 paired ESCC and adjacent normal tissues (right panel), showing that the *LAMP3* mRNA level increases in ESCC samples relative to paired normal counterparts. **(B)** IHC staining for LAMP3 was performed in 77 pairs of ESCC tissues and adjacent normal tissues. The representative images of one pair of tissues are presented here. Scale bar, 100 μm. **(C)** The IHC score of LAMP3 shows that *LAMP3* protein levels are markedly higher in ESCC tissues than in adjacent normal tissues (N=77). **(D)** The expression of *LAMP3* in ESCC patients with positive or negative LNM (GSE47404) demonstrates that it increases in primary tumors from the former patients relative to that in the latter patients. **(E)** IHC staining for LAMP3 in metastasis–positive (N=8) or metastasis-negative (N=15) lymph nodes of patients with ESCC was performed. Representative images of the two groups are showed. Scale bar, 100 μm. **(F)** The protein levels of *LAMP3* in negative lymph nodes (N=8) or positive lymph nodes (N=15) were compared, showing that LAMP3 is increased in metastatic lesions in positive lymph nodes. *P<0.05, **p < 0.01, ****p < 0.0001.

Fig. 2 LAMP3 promotes the migration and invasion of ESCC cells *in vitro*. **(A and B)** Establishment of stable *LAMP3* knockdown in 30-D-4 (A) and K450LM2 (B) cells. LAMP3 protein levels were measured by western blot. GAPDH was used as the

loading control. **(C and D)** Establishment of stable *LAMP3*-overexpressing KYSE30 cells (C) and KYSE450 cells (D). The protein levels of *LAMP3* were examined by western blot. GAPDH was used as the loading control. **(E and F)** Transwell assays were performed to unveil the inhibitory effect of *LAMP3* knockdown on the motility of 30-D-4 and K450LM2 cells. Representative results of three independent assays are shown in E and F (left panel). Scale bar, 200μm. The results were quantitatively analyzed for 30-D-4 and K450LM2 cells (E and F, right panel). **(G and H)** The motility capacity of *LAMP3*-overexpressing KYSE30 or KYSE450 cells was significantly promoted compared to that of the control cells. Representative results of three independent assays are presented (G and H, left panel). Scale bar, 200μm. The numbers of penetrated cells were counted, and the significance was evaluated (G and H, right panel). **p < 0.01, ***p < 0.001, ****p < 0.0001.

Fig. 3 LAMP3 drives lymph node and distal lung metastasis *in vivo*. **(A)** Bioluminescent imaging (left panel) and quantification of photon flux (right panel) of lung metastatic tissues from SCID-Beige mice with intravenous injection of the indicated cells. LAMP3 knockdown markedly inhibited the pulmonary metastasis of ESCC cells. **(B)** Representative H&E staining of the dissected lungs from the SCID-Beige mice in the indicated group is presented (N=6 mice per group), showing that shCtrl 30-D-4 cells gave rise to more and larger metastases than shLAMP3#4/#6 cells. Scale bar, 1 mm. **(C)** Representative image of a dissected popliteal LN. The indicated cells were injected into the foot pads of Balb/c nude mice, and their popliteal LNs

were harvested and examined after 10 weeks. **(D)** The sizes and weights of popliteal LNs (N=8) were quantified and analyzed, demonstrating that shCtrl LNs were larger than the shLAMP3#4/#6 counterparts (left panel). Consistently, these LNs in the shCtrl group were heavier than those in the two LAMP3-depleted groups (right panel). **(E)** Histological examination of popliteal LNs with H&E staining. Representative results of the indicated groups are shown. Scale bar, 1 mm. **(F)** All popliteal LNs in the shCtrl mice were metastatic positive, while the positive ratio decreased to 37.5% in shLAMP3#4 mice and to 50% in shLAMP3#6 mice ($p = 0.0239$). $^{**}p < 0.01$, $^{***}p < 0.001$, $^{****}p < 0.0001$.

Fig. 4 VASP is phosphorylated at Ser239, which blocks motility in LAMP3-depleted ESCC cells. **(A and B)** In the chemotaxis culture model, 30-D-4/K450LM2 cells with stable LAMP3 knockdown (A) or KYSE30/KYSE450 cells with LAMP3 overexpression (B) were seeded into inserts of 6-well transwell plates with bottom chambers filled with 20% FBS-containing RPMI 1640 medium. Cell lysates were collected after 2 h of chemotaxis and then subjected to western blot analysis, showing that depletion of LAMP3 increased the level of phosphorylated VASP(Ser239), while overexpression of *LAMP3* decreased the level of this phosphorylated protein at Ser239. Here are shown representative results of three independent assays. **(C-F)** Knockdown of VASP in 30-D-4 cells was verified by western blot (C). GAPDH was used as the loading control. The control and VASP-depleted 30-D-4 cells (D) were subjected to transwell assays. Representative transwell images of three independent assays are shown in D (left

panel). The numbers of penetrated shVASP 30-D-4 cells increased dramatically relative to the shCtrl counterparts (D, right panel). Similar results were obtained in K450LM2 cells based on three independently repeated experiments (E and F) Scale bar, 200μm. **(G-J)** Western blot analysis showed that LAMP3 and VASP were efficiently depleted simultaneously in 30-D-4 cells (G). VASP depletion significantly restored the *in vitro* motility capacity of 30-D-4 (H) cells depleted of LAMP3. Similar results were obtained in K450LM2 cells (I and J). All the rescue assays were repeated three times independently. Scale bar, 200μm. **p < 0.01, ***p < 0.001, ****p < 0.0001.

Fig. 5 Phosphorylation of Ser239 on VASP is required for the inhibitory effect of LAMP3 depletion on ESCC cell motility and metastasis. **(A-D)** LAMP3-depleted 30-D-4 cells were forced to overexpress with VASP(WT) and VASP(S239A) (A). Western blotting verified that the levels of phosphorylated VASP(Ser239) increased dramatically in shLAMP3/VASP(WT) 30-D-4 cells under chemotactic conditions, while this phosphorylated VASP failed to increase in cells overexpressing VASP(S239A). Representative *in vitro* migration and invasion results of 30-D-4 cells are presented (B, left panel), showing that VASP(S239A) could restore the motility capacity of shLAMP3 cells. The penetrated 30-D-4 cells in each group were counted from three randomly selected fields (B, right panel). Similar results were consistently observed in K450LM2 cells (C and D). All the rescue assays were repeated three times independently. Scale bar, 200μm. **(E)** The popliteal LNs in the indicated four groups

were photographed and weighed (N=6 mice per group), demonstrating that the LNs in the shLAMP3/VASP(S239A) group were larger and heavier relative to those in cells with LAMP3 depletion only. **(F)** Representative images of H&E staining of popliteal LNs in the indicated groups. Scale bar, 300 μm. **(G)** LAMP3 deficiency reduced the LNM ratio in shLAMP3/pLVX and shLAMP3/VASP(WT) cells compared to that in shCtrl/pLVX cells, whereas the LNM ratio reached 100% due to overexpression of VASP(S239A) in 30-D-4 LAMP3-depleted cells. *p < 0.05, **p < 0.01, ***p < 0.001, ****p < 0.0001.

Fig. 6 PKA-mediated VASP phosphorylation at Ser239 represses ESCC cell motility *in vitro*. **(A)** PKA inhibitor H 89 2HCL (10 μM) and AC inhibitor SQ22536 (100 μM) treatment enhanced the invasive capacity of 30-D-4 cells. The AMPK inhibitor dorsomorphin (10 μM) and the soluble AC inhibitor bithionol (50 μM) exerted inhibitory effects on the motility of 30-D-4 cells. DMSO acted as a vehicle control. The invasive abilities of the cells from the indicated 15 groups were tested simultaneously. Representative transwell results of three independent assays are presented in the left panel. The penetrated cells in the indicated groups were counted from three randomly selected fields (right panel). Scale bar, 200μm. **(B)** The phosphorylation level of VASP at Ser239 was examined by western blot after LAMP3-depleted 30-D-4 cells were treated with H 89 2HCL (10 μM) or SQ22536 (100 μM) in a chemotaxis model, showing that both inhibitors impeded the activation of phosphorylated VASP(Ser239) in shLAMP3 30-D-4 cells. In order to acquire blotting

images with better quality, 20 μg proteins of the DMSO-treated cells and 40 μg proteins of the two inhibitors-treated cells were subjected to SDS-PAGE, respectively. Representative western blotting results of three independent experiments are presented. **(C and D)** Double depletion of two PKA regulatory subunits (PRKAR1A and PRKAR2A) in LAMP3-depleted 30-D-4 cells significantly decreased VASP phosphorylation at Ser239 (C), which increased the motility of LAMP3-depleted 30-D-4 cells (D). Representative images are presented in the left panel of D. Three randomly selected fields were subjected to statistical analysis (D, right panel). Scale bar, 200μm. **(E and F)** Knockdown of two PKA regulatory subunits (PRKAR1A and PRKAR2A) in LAMP3-depleted K450LM2 cells showed similar results as those in 30-D-4 cells. Scale bar, 200μm. All the rescue assays (**C-F**) were repeated three times independently. *$p < 0.05$, **$p < 0.01$, ***$p < 0.001$, ****$p < 0.0001$.

Figure 7. Schematic diagram of one mechanism underlying how LAMP3 promotes ESCC metastasis. In a chemotaxis model, depletion of LAMP3 activates the local PKA, which in turn phosphorylates VASP at Ser239 and accordingly markedly suppresses the motility of ESCC cells *in vitro* and metastasis *in vivo*.

Supplemental Figure 1 **(A and B)** *LAMP3* expression was increased in ESCC cell sublines with enhanced motility capacity. RT-qPCR detection of *LAMP3* expression in parental KYSE30 cells versus 30-D-4 cells (A, left panel) or KYSE450 cells versus K450LM2 cells (B, left panel). *LAMP3* protein levels were also detected using western

blotting in parental KYSE30 versus 30-D-4 cells (A, right panel) or KYSE450 versus K450LM2 cells (B, right panel). **(C and D)** The mRNA levels of *LAMP3* were significantly decreased using specific shRNA oligos in 30-D-4 (C) or K450LM2 (D) cells. **(E and F)** The mRNA levels were increased in LAMP3-KYSE30 (E) and LAMP3-KYSE450 (F) cells relative to their pLVX counterparts. **(G and H)** Wound healing assays showed that *LAMP3* knockdown inhibited migration in 30-D-4 (G) and K450LM2 (H) cells. The wounded regions were imaged at 0 h and 36 h. The quantified evaluations of healing rates of 30-D-4 or of K450LM2 cells are presented in G (right panel) and H (right panel), respectively. The wound healing assays were independently performed three times and here are shown the representative results. *$p < 0.05$, ***$p < 0.001$.

Supplemental Figure 2 **(A and B)** CCK-8 assays were performed in shLAMP3#4/#6 and shCtrl 30-D-4 (A) or K450LM2 (B) cells, showing that LAMP3 depletion did not affect the viability of ESCC cells. CCK-8 reagent was added to each well (N=5 wells per group) at 0, 1, 2, and 3 d. The absorbance at 450 nm was measured after incubation for 2 h at 37°C. Three independent CCK-8 assays were performed and the representative data are shown here as the mean ± S.D. **(C)** The harvested xenografts arising from the subcutaneously injected shCtrl and shLAMP3#4 30-D-4 cells are presented (N=5 in each group). **(D)** Growth curves of shCtrl and shLAMP3#4 tumors are plotted, demonstrating that the tumor volumes between the two groups remained comparable during the experiment. **(E)** Tumor masses from the shCtrl and shLAMP3#4 groups were weighed, and no significant difference was observed. These

data are presented as the mean ± S.D.

Supplemental Figure 3 **(A)** Representative images of the harvested lungs from the shCtrl, shLAMP3#4, and shLAMP3#6 group. **(B)** The numbers of lung metastatic nodes were counted, showing that LAMP3 depletion markedly attenuated the formation of pulmonary metastases *in vivo*. ****p < 0.0001.

Supplemental Figure 4. Western blotting assays were independently performed three times to examine the levels of the phosphorylated VASP at Ser157 and Ser239 in LAMP3-depleted 30-D-4 (**A**) and K450LM2 (**B**) cells under adherent conditions. The representative results show that reduced LAMP3 did not change the levels of p-VASP (Ser157) and p-VASP (Ser239) in both cell lines.

Figure 1

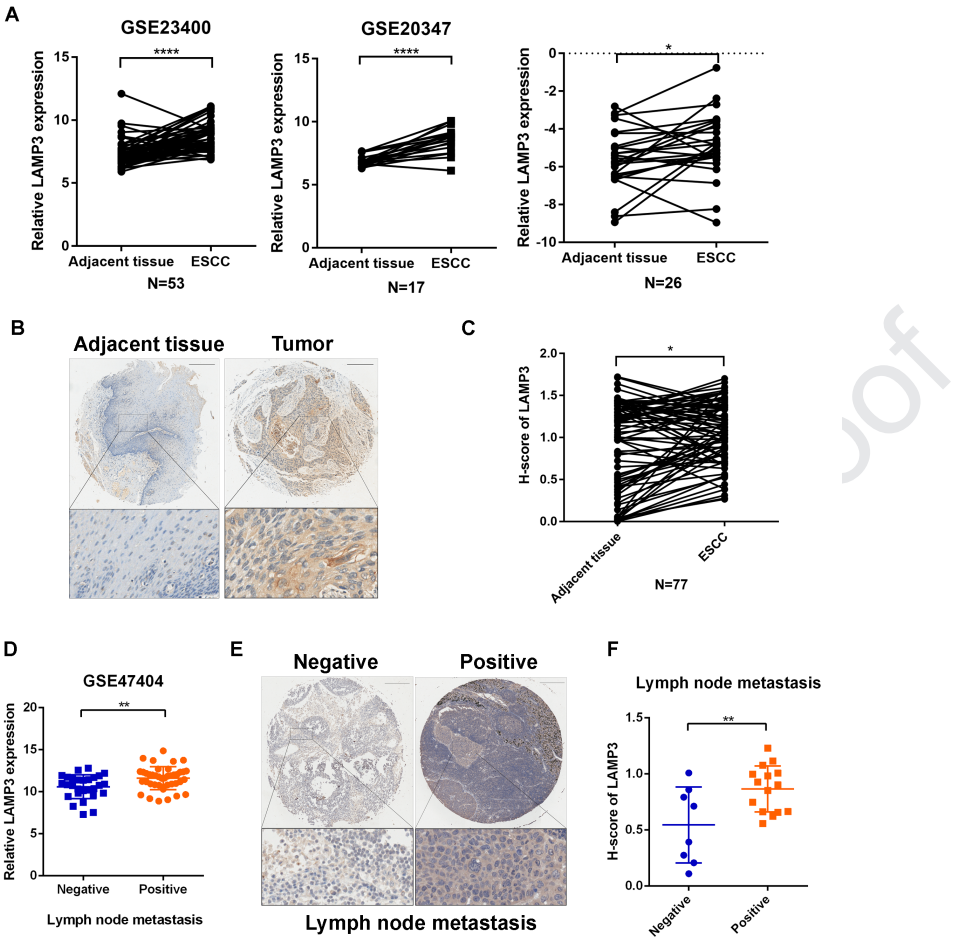
A
GSE23400
****
Relative LAMP3 expression
15
10
5
0
Adjacent tissue
ESCC
N=53
GSE20347
****
Relative LAMP3 expression
15
10
5
0
Adjacent tissue
ESCC
N=17
*
Relative LAMP3 expression
0
-2
-4
-6
-8
-10
Adjacent tissue
ESCC
N=26
B
Adjacent tissue
Tumor
C
*
H-score of LAMP3
2.0
1.5
1.0
0.5
0.0
Adjacent tissue
ESCC
N=77
D
GSE47404
**
Relative LAMP3 expression
20
15
10
5
0
Negative
Positive
Lymph node metastasis
E
Negative
Positive
Lymph node metastasis
F
Lymph node metastasis
**
H-score of LAMP3
1.5
1.0
0.5
0.0
Negative
Positive

Figure 2

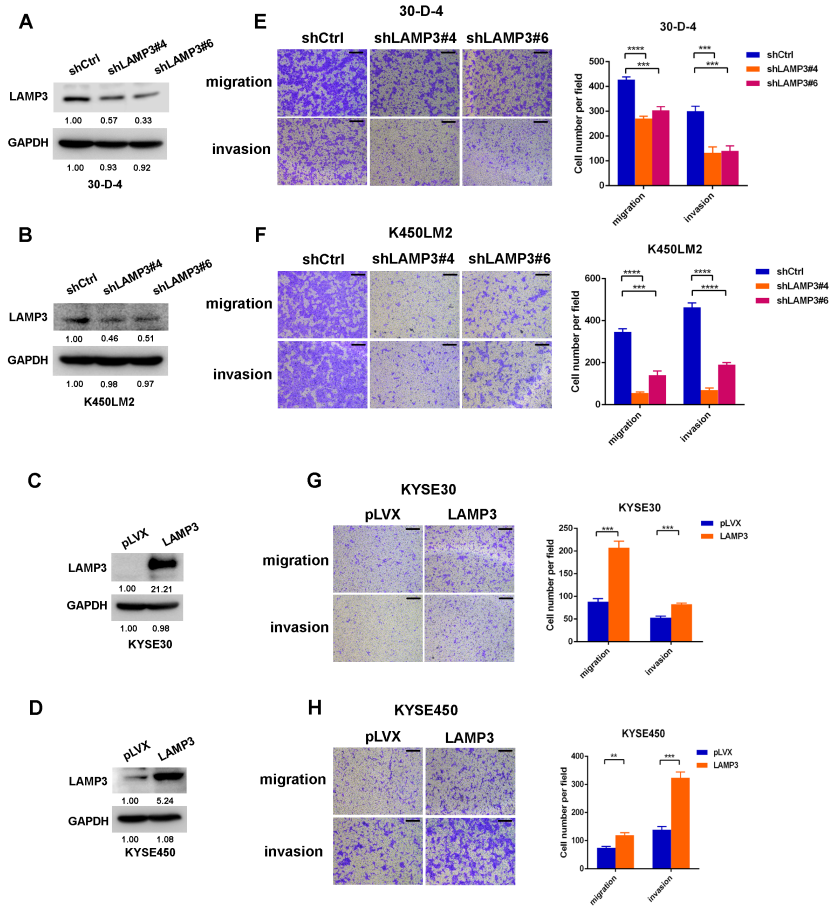
A
shCtrl
shLAMP3#4
shLAMP3#6
LAMP3
1.00 0.57 0.33
GAPDH
1.00 0.93 0.92
30-D-4
B
shCtrl
shLAMP3#4
shLAMP3#6
LAMP3
1.00 0.46 0.51
GAPDH
1.00 0.98 0.97
K450LM2
C
pLVX
LAMP3
LAMP3
1.00 21.21
GAPDH
1.00 0.98
KYSE30
D
pLVX
LAMP3
LAMP3
1.00 5.24
GAPDH
1.00 1.08
KYSE450
E
30-D-4
shCtrl
shLAMP3#4
shLAMP3#6
migration
invasion
30-D-4
shCtrl
shLAMP3#4
shLAMP3#6
Cell number per field
migration
invasion
F
K450LM2
shCtrl
shLAMP3#4
shLAMP3#6
migration
invasion
K450LM2
shCtrl
shLAMP3#4
shLAMP3#6
Cell number per field
migration
invasion
G
KYSE30
pLVX
LAMP3
migration
invasion
KYSE30
pLVX
LAMP3
Cell number per field
migration
invasion
H
KYSE450
pLVX
LAMP3
migration
invasion
KYSE450
pLVX
LAMP3
Cell number per field
migration
invasion

Figure 3

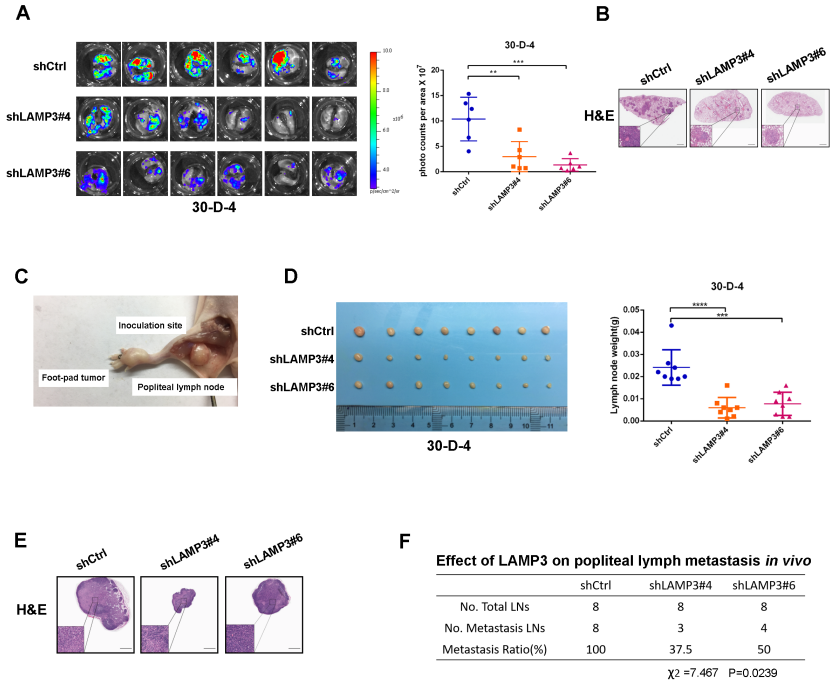

F

Effect of LAMP3 on popliteal lymph metastasis *in vivo*

	shCtrl	shLAMP3#4	shLAMP3#6
No. Total LNs	8	8	8
No. Metastasis LNs	8	3	4
Metastasis Ratio(%)	100	37.5	50

χ^2 =7.467 P=0.0239

Figure 4

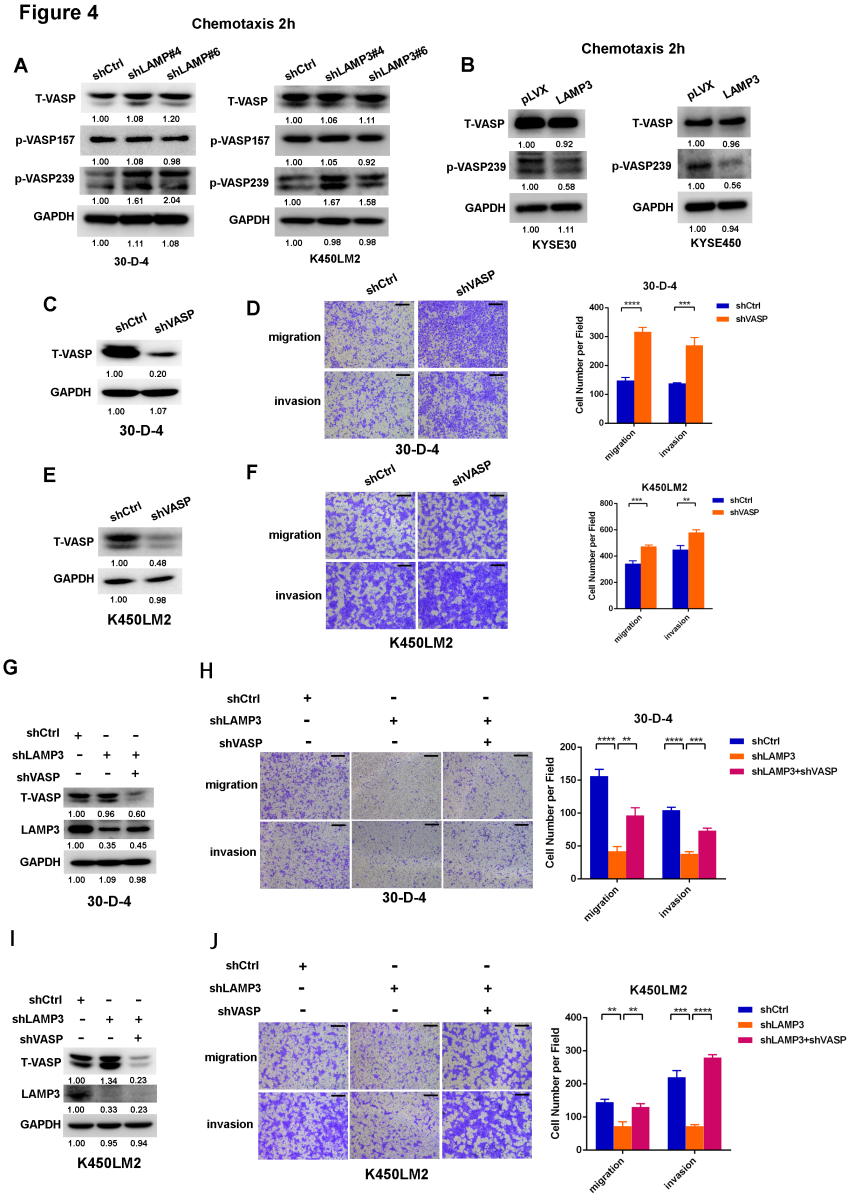
Chemotaxis 2h
A
shCtrl
shLAMP#4
shLAMP#6
T-VASP
p-VASP157
p-VASP239
GAPDH
30-D-4
shLAMP3#4
shLAMP3#6
K450LM2
Chemotaxis 2h
B
pLVX
LAMP3
KYSE30
KYSE450
C
shVASP
D
migration
invasion
E
F
G
shLAMP3
shVASP
LAMP3
H
Cell Number per Field
shLAMP3+shVASP
I
J

Figure 5

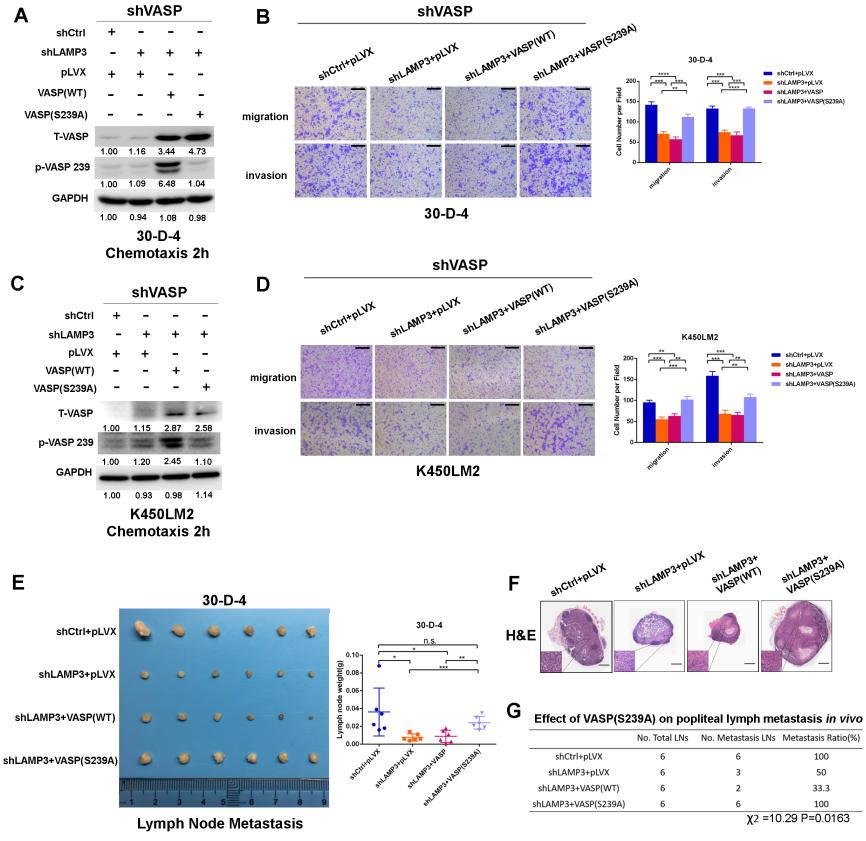

G **Effect of VASP(S239A) on popliteal lymph metastasis *in vivo***

	No. Total LNs	No. Metastasis LNs	Metastasis Ratio(%)
shCtrl+pLVX	6	6	100
shLAMP3+pLVX	6	3	50
shLAMP3+VASP(WT)	6	2	33.3
shLAMP3+VASP(S239A)	6	6	100

χ^2 =10.29 P=0.0163

Figure 6

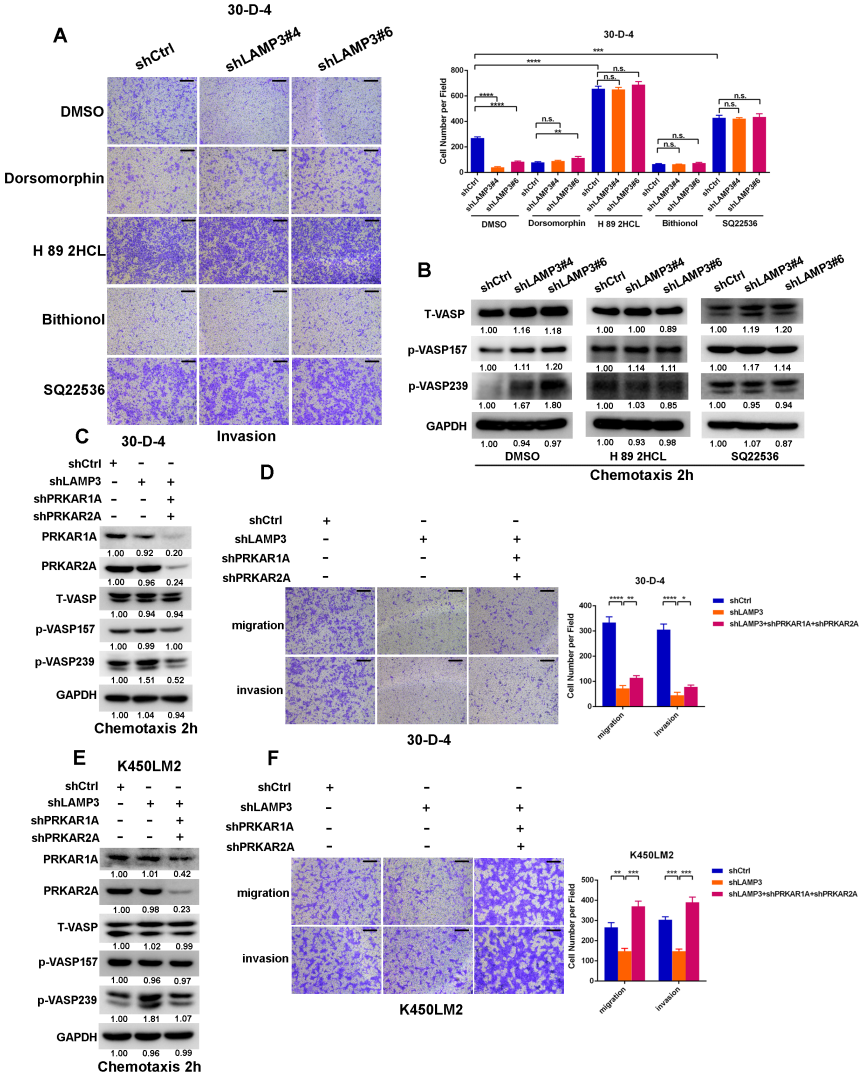
A
30-D-4
shCtrl
shLAMP3#4
shLAMP3#6
DMSO
Dorsomorphin
H 89 2HCL
Bithionol
SQ22536
Invasion
30-D-4
Cell Number per Field
DMSO
Dorsomorphin
H 89 2HCL
Bithionol
SQ22536
B
T-VASP
p-VASP157
p-VASP239
GAPDH
Chemotaxis 2h
C
30-D-4
shCtrl
shLAMP3
shPRKAR1A
shPRKAR2A
PRKAR1A
PRKAR2A
T-VASP
p-VASP157
p-VASP239
GAPDH
Chemotaxis 2h
D
migration
invasion
30-D-4
shLAMP3+shPRKAR1A+shPRKAR2A
E
K450LM2
Chemotaxis 2h
F
K450LM2

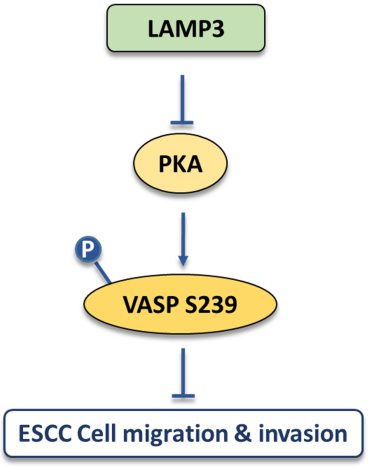
LAMP3
PKA
P
VASP S239
ESCC Cell migration & invasion

- Highlights

  - Overexpressed *LAMP3* positively correlates with lymph node metastasis in ESCC.
  - LAMP3 promotes ESCC metastasis by attenuating VASP phosphorylation at Ser239.
  - PKA specifically phosphorylates VASP at Ser239 to inhibit ESCC metastasis.

Conflicts of interest

No potential conflicts of interest were disclosed.